Hindawi
Journal of Advanced Transportation
Volume 2021, Article ID 8380247, 15 pages
https://doi.org/10.1155/2021/8380247

Research Article

Research on the Evolution Mechanism of Congestion in the Entrances and Exits of Parking Facilities Based on the Improved Spatial Autoregressive Model

Hongru Yu,[1] **Shejun Deng**,[1] **Caoye Lu**,[1] **Yucheng Tang**,[1,2] **Shijun Yu**,[1] **Lu Liu**,[1] **and Tao Ji**[1]

[1]*College of Civil Science and Engineering, Yangzhou University, Yangzhou 225002, China*
[2]*China Iconic Technology Company Limited, Hefei 230088, China*

Correspondence should be addressed to Shejun Deng; yzrx6@163.com

Received 18 June 2021; Revised 1 August 2021; Accepted 13 August 2021; Published 30 August 2021

Academic Editor: Jinjun Tang

The entrance and exit area of parking facilities has the characteristics of high concentration of urban traffic and prominent traffic intertwining phenomenon, which easily induces rapid congestion of mixed heterogeneous traffic at specific times and local locations and quickly spreads to the entire road section or even a larger area. In order to better understand the congestion distribution characteristics and propagation effects of access section of the parking entrance and exit from the mid and microperspective, a 5 m ∗ lane width pixel grid is used to divide the frontage road research. It also proposes a spatially robust autoregressive model and complex network tools suitable for analysis of local traffic flow to analyze it. The results show that as spatial scale increases, the congestion propagation decreases sharply and spatial adjacency within the fourth order can account for more than 90% of the propagation; the frontage road to the entrance and exit is the place where the congestion first happens, and the congestion gradually attenuates as it propagates to the inner lane and the upstream of the road segments; the lateral congestion propagation attenuates faster, so the area affected by congestion is mainly distributed in the outermost lane. This paper can provide theoretical guidance for alleviating traffic congestion in the entrance and exit areas of parking facilities and has theoretical and empirical significance.

1. Introduction

Increasing car park [1], which exacerbates the contradiction between the supply and demand of urban parking, along with the lag of parking facilities planning [2–4] and other factors, causes more severe traffic congestion problems in the entrances and exits of parking facilities. Since the entrances and exits of parking facilities are generally set up on secondary arterial roads or branch roads with low capacity, the interweaving of incoming and outgoing vehicles with external traffic will reduce the traffic capacity [5, 6], increase the delay time of main road traffic [7, 8], and even cause a bottleneck and congestion on the upstream road.

At present, research focused on the traffic conditions in entrances and exits of the off-street parking is still very rare. Previous research mainly focuses on the complex impact of the bus stop [9–14] and on-street parking [15–18] on the traffic flow. Compared with other road facilities, the settings of entrances and exits of parking facilities can bring more complicated impact: on the one hand, due to the uncertainty of the occurrence and attraction of parking facilities, the temporal and spatial distribution of parked vehicles are more disorderly; the intermittently concentrated entering and departing of vehicles enhance the occasional disturbance to the road; on the other hand, the interwoven flow of incoming and outgoing vehicles, the traffic flow of the main road, and the flow of motor vehicles and nonmotorized vehicles [19] increase the heterogeneity of the traffic flow and the complexity of the occurrence of congestion in this area to a certain extent.

In the analysis of traffic congestion, scholars have built various models to reveal the essence of congestion. At the macrolevel [20–24], traffic congestion is generally regarded as a process of compression, blockage, and spread of traffic

flow. At the microlevel [25–29], more attention is paid to conflicts, queuing, and easing of vehicles. Spatial autocorrelation is a geographic concept, which refers to the potential interdependence between observed data of some variables in the same distribution area [30, 31]. The development of this theory in the field of transportation has resulted in its wide use in traffic feature recognition [32] at the macrolevel and mid level and accident analysis [33–36]. In addition, complex network theory, as a new scientific theory for revealing network complexity phenomena, has a wide range of applications for the organization and optimization of transportation logistics [37–40] and the macrointerpretation of transportation systems [41–46], but it is rarely used in the study of traffic flow characteristics at the meso-microlevels.

To sum up, although there are rich research outcomes on congestion propagation, research on the frontage roads of parking facilities is still relatively rare; besides, although the spatial autocorrelation theory has developed in the field of transportation, due to its higher requirements on spatial stability, it is not suitable for the research of transportation theory at the mid and microlevel. In response to the abovementioned problems, improving the spatial autocorrelation model, building a model of the spatial congestion propagation in the entrances and exits of the parking facilities from the mid and microperspective under the guidance of the complex network theory and other theories, and exploring the attenuation effect and key nodes in the process of congestion propagation based on the observed data are of great significance for alleviating traffic congestion in the entrances and exits of parking facilities.

2. Data Description

In order to determine the objective of the study, the frontage road of this article is defined as follows: the free road segments from about 140 m upstream to about 20 m downstream from the entrance and exit access points. This paper selects the entrance and exit of the parking lot of the West Affiliated Hospital of Yangzhou University as a typical off-street parking area. The frontage road is the one-way three-lane road (a part of the two-way six-lane road with a separation zone in the middle), and the upstream area is far away from the intersection. The traffic volume and entry rate vary significantly in different periods, and the road segment is free of vegetation, billboards, and other structures, which are conducive for data collection. The data set in this paper is obtained by aerial filming, with a wind-proof drone MAVIC_AIR2 recording the traffic conditions in the experimental area at an altitude of 100–150 m (each video lasts 10–15 minutes, 100 videos in total). Then, the open-source vehicle-tracking algorithm based on YOLOV5 and DeepSort [47] is used to monitor the location parameters of the moving vehicle [48, 49] in real time (as shown in Figure 1).

In order to describe the location of the lanes in an easy way, the lanes in the experimental area are numbered, where the outermost lane is Lane 3, the middle lane is Lane 2, and the innermost lane is Lane 1. In addition, in order to study the relationship of the traffic state of each spatial unit in the entrance and exit and the spatial congestion propagation, this paper divides the road into three lanes and then further divides these three lanes into 5-meter wide spatial units, which can ensure the spatial accuracy of the model and meet the requirements of velocity measurement, as shown in Figure 2.

The investigation finds that the time for vehicles to enter the parking lot is generally within the range of 3 to 13 seconds. In order to extract the traffic information of each spatial unit to the greatest extent, this paper uses a time interval of 3 seconds to calculate the average speed of vehicles in each spatial unit. The sample data are shown in Table 1.

3. Method

3.1. Improved Spatial Autoregressive Model. The traditional spatial autoregressive model requires the data to have spatial stability. However, due to the influence of external factors such as the actual environment and traffic conditions, the spatial stability of the measured data is often poor. In order to reduce the influence of external factors on the modeling results, this paper improves the traditional spatial autoregressive model and builds a robust spatial autoregressive model based on repeated observation data that consider spatial instability and multiple correlations.

The traditional spatial autoregressive model adds a spatial lag term to the general regression model, that is, the dependent variable of a spatial object is related to the independent variable on the same object, and it is also related to the independent variable and dependent variable of adjacent objects. Its general form is shown in

$$\begin{cases} z = \rho W_1 z + X\beta + \mu, \\ \mu = \lambda W_2 \mu + \varepsilon, \\ \varepsilon \sim N\left(0, \sigma^2 I\right). \end{cases} \tag{1}$$

Here, z represents the spatial attributes of the research object, or the dependent variable; X represents the spatial attribute of the adjacent objects, or the independent variable; ρ is the spatial autoregressive coefficient; β is the regression coefficient; μ represents the residual of the model; λ represents the residual spatial regression coefficient; ε represents the random error; and W_1 and W_2 represent the spatial adjacency matrix of the spatial units of frontage road.

Observing the influencing factors of the attribute value of the spatial unit in the study area, it is not difficult to find that the change of the attribute value of the spatial unit is mainly affected by the adjacent spatial unit, while the explanatory variable X has almost no contribution. Therefore, X and W_2 in formula (1) can be assigned to 0, and the first-order spatial autoregressive model can be obtained, as shown in

$$\begin{cases} z = \rho W_1 z + \varepsilon, \\ \varepsilon \sim N\left(0, \sigma^2 I\right). \end{cases} \tag{2}$$

In order to study the propagation mechanism of congestion at different spatial scales, this paper divides adjacent spatial units according to "distance" and takes the influence

Figure 1: Vehicle tracking.

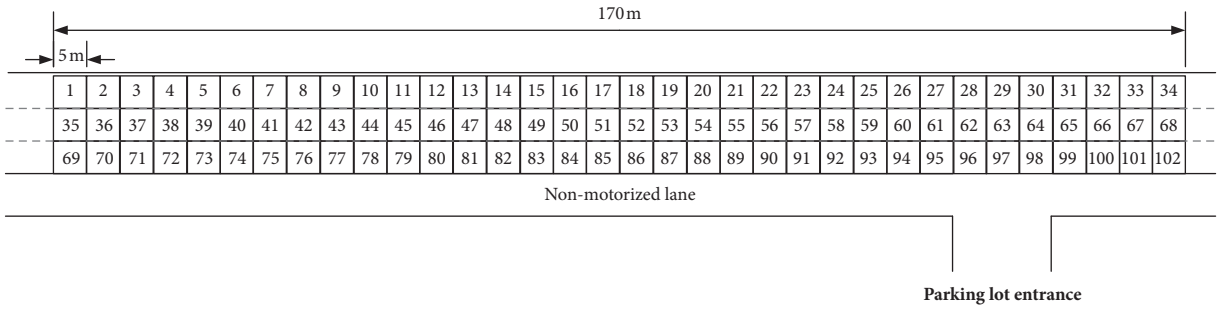

Figure 2: Grid division of road sections.

Table 1: Samples of average speeds of spatial units (unit: km/h).

Spatial unit	Time					
	1	2	3	4	...	110
	0 s–3 s	3 s–6 s	6 s–9 s	9 s–12 s	...	327 s–330 s
1	41.46	41.21	41.03	43.82	...	35.78
2	41.11	40.99	40.84	44.02	...	35.56
3	40.80	40.85	40.98	44.15	...	35.39
4	40.46	40.83	41.12	44.27	...	35.23
...	...	...	...	...	...	...
102	45.12	44.93	44.46	44.46	...	40.45

of spatial units under each adjacent number on the research object as an independent variable. Taking into account the correlation between the independent variables, the direct use of traditional parameter estimation methods based on the least squares method will cause larger errors. Therefore, this paper proposes an improved first-order spatial autoregressive model that takes into account spatial instability and multiple correlations.

In the improved spatial autoregressive model, the disturbance of the research object is the dependent variable and the disturbances of other spatial units are the independent variables to describe the relationship between the spatial units in the research attributes, as shown in formula

$$y' = \sum_{k=1}^{K} \rho_k \overline{W}^k y' + \gamma l + \varepsilon. \tag{3}$$

Here, y' represents the velocity disturbance sequence of the research object; $\overline{W}^k$ represents the k-order spatial adjacency matrix considering spatial instability; ε represents the error term of the improved spatial autoregressive model; l is the constant term; ρ_k represents the spatial lag term; the regression coefficient of $\overline{W}^k$; γ represents the regression coefficient of the constant term; k represents the number of spatial adjacencies; and K is the maximum number of spatial adjacencies considered.

For the space unit under study, the historical sequence of the previous c cycle formula (4) can be constructed to obtain the velocity sequence of each space unit:

$$Y = \begin{bmatrix} y_{1,1} & y_{2,1} & \cdots & y_{n-1,1} & y_{n,1} \\ y_{1,2} & y_{2,2} & & y_{n-1,2} & y_{n,2} \\ \vdots & & \ddots & \vdots & \\ y_{1,c} & y_{2,c} & \cdots & y_{n-1,c} & y_{n,c} \end{bmatrix}. \tag{4}$$

Here, y_i represents the data of space unit i in c cycles and $y_i = [y_{i,1}, y_{i,2}, y_{i,3}, \ldots, y_{i,c}]^T$ is the speed history data sequence of space unit i.

3.1.1. Speed Disturbance Sequence. "Urban Traffic Management Evaluation Index System" (2002, China) stipulates that when the average speed of motor vehicles on the main road is not less than 30 km/h, the road is unblocked. Therefore, the speed perturbation sequence of the unit of the space is calculated according to the speed history data sequence. As shown in formulas (5) and (6), y_i is the historical velocity sequence of space unit i and $\widehat{y}$ is the historical velocity perturbation sequence:

$$y' = \widehat{y} = \left[\widehat{y}_1, \widehat{y}_2, \widehat{y}_3, \ldots, \widehat{y}_n\right]^T, \tag{5}$$

$$\widehat{y}_i = -\left(y_i - 30\right). \tag{6}$$

3.1.2. Considering the Spatial Adjacency Matrix That Is Not Stationary. The traditional spatial adjacency matrix based on the boundary adjacency method or the center-of-gravity distance method assumes that all adjacent objects have the same weight value, which is inconsistent with the actual situation of congestion propagation. On the one hand, the number of adjacencies in different spatial units is different. On the other hand, the traffic flow is not homogenous and the effects of adjacent units in different directions are not the same.

The spatial adjacency matrix determined based on the boundary adjacency method is shown in formulas (5) and (6). In the formula, $w_{i,j}^k$ indicates that there is a k-order adjacency relationship between space unit i and space unit j. Determining the spatial adjacency matrix based on the boundary adjacency method is a commonly used method to determine the adjacency relationship between area units; if two spatial units have the same boundary, they have a first-order spatial adjacency relationship and the k-order adjacency relationship can be determined according to the transitivity of the spatial adjacency relationship.

$$W^k = \begin{bmatrix} w_{1,1}^k & w_{1,2}^k & \cdots & w_{1,j}^k & \cdots & w_{1,n}^k \\ w_{2,1}^k & w_{2,2}^k & \cdots & w_{2,j}^k & \cdots & w_{2,n}^k \\ w_{i,1}^k & w_{i,2}^k & \cdots & w_{i,j}^k & \cdots & w_{i,n}^k \\ \cdots & \cdots & \cdots & \cdots & \cdots & \cdots \\ w_{n,1}^k & w_{n,2}^k & \cdots & w_{n,j}^k & \cdots & w_{n,n}^k \end{bmatrix},$$
$$w_{i,j}^k = \begin{cases} 1, & i \text{ and } j \text{ have } k-\text{order adjacency}, \\ 0, & i \text{ and } j \text{ do not have } k-\text{order adjacency}. \end{cases} \tag{7}$$

In order to accurately describe the relationship between the spatial units, first, according to the spatial adjacency matrix W^k, determine the set of spatial units that have a k-order adjacency relationship with each spatial unit, denoted as $f_k(i, j), j = 1, 2, 3, \ldots, r, \ldots, R$; then, the rth space unit that has an adjacency relationship of order k with the space unit i is denoted as $f_k(i, r)$.

Let vector $\widehat{y}_i = [\widehat{y}_{i,1}, \widehat{y}_{i,2}, \widehat{y}_{i,3}, \ldots, \widehat{y}_{i,r}, \ldots, \widehat{y}_{i,R}]^T$ be the velocity history perturbation sequence of space unit i, and H_i^k is the matrix of velocity history perturbation sequences of all space units that have a k-order adjacency relationship with space unit i, as shown in

$$H_i^k = \left[\widehat{y}_{f_k(i,1)}, \widehat{y}_{f_k(i,2)}, \widehat{y}_{f_k(i,3)}, \ldots, \widehat{y}_{f_k(i,r)}, \ldots, \widehat{y}_{f_k(i,R)}\right]. \tag{8}$$

In order to preserve the features in H_i^k to the greatest extent and reduce their dimensionality, the principal component analysis method is used to extract the first principal component that is most similar to the velocity history disturbance sequence $\widehat{y}_i$ of space unit i from H_i^k.

Let the vector $\widehat{u}_i^k = [u_{f_k(i,1)}^k, u_{f_k(i,2)}^k, u_{f_k(i,3)}^k, \ldots, u_{f_k(i,r)}^k, \ldots, u_{f_k(i,R)}^k]^T$ be the weight value of each spatial unit that has a kth order adjacency with the spatial unit i, in order to ensure each weight value can accurately describe the degree of association between spatial units, and the covariance between $H_i^k\widehat{u}_i^k$ and $\widehat{y}_i$ should be the largest, as shown in

$$\max\left(H_i^k\widehat{u}_i^k\right)^T\widehat{y}_i. \tag{9}$$

Use the Lagrangian method to solve the model, as in formula (9):

$$F = \left(H_i^k\widehat{u}_i^k\right)^T\widehat{y}_i - \lambda\left(\widehat{u}_i^{kT}\widehat{u}_i^k - 1\right). \tag{10}$$

Calculate the partial derivative of F with $\widehat{u}_i^k$ and λ, as shown in

$$\frac{\partial F}{\partial \widehat{u}_i^k} = H_i^{kT}\widehat{y}_i - 2\lambda\widehat{u}_i^k, \tag{11}$$

$$\frac{\partial F}{\partial \lambda} = -\left(\widehat{u}_i^{kT}\widehat{u}_i^k - 1\right). \tag{12}$$

According to formula (12),

$$\widehat{u}_i^k = \frac{H_i^{kT}\widehat{y}_i}{\left\|H_i^{kT}\widehat{y}_i\right\|}. \tag{13}$$

The value $u_{f_k(i,r)}^k$ in $\widehat{u}_i^k$ represents the spatial association relationship of the rth spatial unit that has a k-order adjacency with the spatial unit i; the sign of $u_{f_k(i,r)}^k$ indicates the positive or negative correlation between the space unit i and the rth space unit that has a k-order adjacency relationship, and the absolute value indicates the relationship between the space units. The greater the correlation, the greater the absolute value, and vice versa. In actual road conditions, the propagation of congestion is the same direction, so only the positive numbers in the vector are retained to construct the smoothed spatial adjacency matrix $\overline{W}^k$, as shown in

$$\overline{W}^k = \begin{bmatrix} \overline{w}_{1,1}^k & \overline{w}_{1,2}^k & \cdots & \overline{w}_{1,j}^k & \cdots & \overline{w}_{1,n}^k \\ \overline{w}_{2,1}^k & \overline{w}_{2,2}^k & \cdots & \overline{w}_{2,j}^k & \cdots & \overline{w}_{2,n}^k \\ \overline{w}_{i,1}^k & \overline{w}_{i,2}^k & \cdots & \overline{w}_{i,j}^k & \cdots & \overline{w}_{i,n}^k \\ \cdots & \cdots & \cdots & \cdots & \cdots & \cdots \\ \overline{w}_{n,1}^k & \overline{w}_{n,2}^k & \cdots & \overline{w}_{n,j}^k & \cdots & \overline{w}_{n,n}^k \end{bmatrix}, \tag{14}$$

$$\overline{w}_{i,j}^k = \begin{cases} 0, & u_{f_k(i,r)}^k \le 0, \\ \dfrac{u_{f_k(i,r)}^k}{\sum_{r=1}^R u_{f_k(i,r)}^k}, & u_{f_k(i,r)}^k > 0. \end{cases} \tag{15}$$

3.2. Parameter Calculation Method. In order to study the spatial propagation process of traffic congestion in the entrance and exit area of parking facilities, in the improved spatial autoregressive model, the disturbance of the research unit is used as the dependent variable and the spatial lag term $\overline{W}^k y'$ of the disturbance under different spatial adjacency k is used as an independent variable; there is a linear correlation between the spatial lag terms $\overline{W}^k y'$ under different spatial adjacency numbers k.

According to the space lag term $\overline{W}^1 y'$ of the disturbance under different number of space delay periods, the independent variable matrix is constructed, as shown in

$$Z(K) = \left[\overline{W}^1 y', \overline{W}^2 y', \overline{W}^3 y', \ldots, \overline{W}^k y', \ldots, \overline{W}^K y'\right]. \tag{16}$$

3.2.1. Improved Spatial Autoregressive Model Parameter Estimation Process. For the convenience of calculation, the dependent variable matrix y' of the improved spatial autoregressive model is marked as F_0, the independent variable matrix is marked as E_0, and the parameter estimation is performed.

Extract the first principal component t_1 from the independent variable matrix, where t_1 is the linear combination of E_0 of the independent variables as shown in formulas (17) and (18). Since the dependent variable contains only one variable, the first principal component of the dependent variable is F_0.

$$t_1 = E_0 u_1, \tag{17}$$

$$u_1 = \left[u_{1,1}, u_{1,2}, \ldots, u_{1,k}\right]^T. \tag{18}$$

For the needs of regression analysis, the extracted principal components must simultaneously meet the requirements of the first principal components t_1 and F_0 of the variables to reflect the characteristics of the variable group to the greatest extent and the correlation between the two first principal components to reach the maximum. Considering the requirements of modeling comprehensively, covariance is selected to characterize the principal components, as shown in

$$\begin{cases} < t_1, F_0 \ge u_1^T E_0^T F_0 \Longrightarrow \max, \\ u_1^T u_1 = 1. \end{cases} \tag{19}$$

According to the Lagrangian multiplier method, the following formula can be obtained:

$$L = u_1^T E_0^T F_0 - \lambda\left(u_1^T u_1 - 1\right). \tag{20}$$

Respectively, find the partial derivatives of u_1 and λ to get the following formulas:

$$\frac{\partial L}{\partial u_1} = E_0^T F_0 - 2\lambda u_1 = 0, \tag{21}$$

$$\frac{\partial L}{\partial \lambda} = -\left(u_1^T u_1 - 1\right) = 0. \tag{22}$$

According to formula (22), we can get

$$\widehat{u}_1 = \frac{E_0^T F_0}{\left\|E_0^T F_0\right\|}. \tag{23}$$

According to the principle of principal component analysis, the sample is expressed as a linear combination of components, that is, regression on t_1 is performed on E_0 and F_0, respectively, as shown in formulas (24) and (25), where E_1 and F_1 are residual matrixes.

$$E_0 = t_1 p_1 + E_1, \tag{24}$$

$$F_0 = t_1 r_1 + F_1. \tag{25}$$

According to (25), the following formulas can be obtained from the least square estimation:

$$\widehat{p}_1 = \frac{E_0^T e_1}{\left\|e_1\right\|}, \tag{26}$$

$$\widehat{r}_1 = \frac{F_0^T e_1}{\left\|e_1\right\|}. \tag{27}$$

Replace E_0 and F_0 with the residual terms E_1 and F_1. Repeat the above steps to obtain the weight vector $\widehat{u}_2$ (formula (28)) of the second principal component t_2 of E_0 and the regression coefficients $\widehat{p}_2$ (formula (29)) and r of E_1 and F_1 with respect to $\widehat{r}_2$ (formula (30)).

$$\widehat{u}_2 = \frac{E_1^T F_1}{\left\|E_1^T F_1\right\|}, \tag{28}$$

$$\widehat{p}_2 = \frac{E_1^T e_2}{\left\|e_2\right\|}, \tag{29}$$

$$\widehat{r}_2 = \frac{F_1^T e_2}{\left\|e_2\right\|}. \tag{30}$$

Assuming that a total of h principal components are extracted, the regression model between F_0 and E_0 can be obtained, as shown in

$$F_0 = e_1\hat{r}_1 + e_2\hat{r}_2 + e_3\hat{r}_3 + \cdots + e_H\hat{r}_H + F_H, \tag{31}$$

$$F_0 = E_0B_0 + F_H, \tag{32}$$

$$B_0 = \hat{r}_1\hat{u}_1^* + \hat{r}_2\hat{u}_2^* + \hat{r}_3\hat{u}_3^* + \ldots\hat{r}_H\hat{u}_H^*, \tag{33}$$

where B_0 is the perturbation sequence F_0 of the dependent variable y' of the improved spatial autoregressive model and the regression coefficient vector between the perturbation matrix E_0 of the independent variable. Determine the value of the regression coefficient according to the position of the respective variable in Z (K). For example, the kth element in B_0 represents the estimated value of ρ_k.

3.2.2. Determination of the Optimal Number of Principal Components. The partial least squares method is a method of establishing a regression model by extracting the principal components of the independent variables. If the number of principal components is too small, the relationship between the variables cannot be reflected; otherwise, overfitting will occur. In order to ensure the validity of the model, the cross-validity criterion is selected to determine the number of principal components to be extracted.

The cross-validity criterion is mainly to test whether the extracted hth principal component can significantly improve the prediction performance of the model compared to the $(h-1)$ th principal component. For the improved spatial autoregressive model, the cross-validity criterion is selected to determine the number of principal components, which is mainly calculated by using all the spatial unit disturbance value sequences to extract the difference between the predicted value and the true value of the spatial unit disturbance when the number of principal components is $(h-1)$. The sum of squared deviations SS_{h-1} is shown in formula (34). And, extract the hth principal component based on the sequence after removing the perturbation value of its own spatial unit and calculate the sum of squared deviations of the predicted value and the true value based on the new sequence PRESS_h, as shown in

$$\mathrm{SS}_{h-1} = \sum_{i=1}^{n}\left(y_t'(i) - \hat{y}_t'(i)\right)^2, \tag{34}$$

$$\mathrm{PRESS}_h = \sum_{i=1}^{n}\left(y_t'(i) - \hat{y}_{t,-i}'(i)\right)^2. \tag{35}$$

According to SS_h and PRESS_h, calculate the effectiveness of extracting the hth principal component Q_h^2 (formula (36)). When $Q_h^2 \geq 1 - 0.95^2$, it indicates that the hth principal component has significantly improved the prediction performance of the model, and it is necessary to continue to extract the principal components; when $Q_h^2 < 1 - 0.95^2$, indicating the introduction after the hth principal component, the model has no obvious improvement, and there is no need to continue to extract principal components.

$$Q_h^2 = 1 - \frac{\mathrm{PRESS}_h}{\mathrm{SS}_{h-1}}. \tag{36}$$

3.3. Improving the Validation of the Spatial Autoregressive Model. For the speed disturbance sequence studied, the improved spatial autoregressive model is used to fit and the model's fitting effect is tested from two aspects: the model's goodness-of-fit (R^2) index and visual observation. When R^2 is closer to 1, it means that the fitting effect is good. On the contrary, when it is close to 0, it means that the fitting effect is poor. When the change trend of the measured value curve and the predicted curve is close, it indicates that the model can reasonably describe the space average speed at each position. On the contrary, it means that the model cannot reasonably reflect the real situation.

3.4. Analysis Method of Congestion Evolution in the Entrance and Exit Area. The improved spatial autoregressive model takes the velocity disturbance of each spatial unit as the dependent variable and independent variable and uses the partial least square method to estimate the parameters of the improved spatial autoregressive model and obtain the parameter estimated value ρ_k under the number of adjacent spaces in each space. The estimated value ρ_k represents the degree of correlation between the degree of velocity disturbance of the k-order adjacent unit of each spatial unit and the degree of correlation between the spatial unit.

Therefore, the parameters in the improved spatial autoregressive model are defined as the propagation structure of each spatial unit velocity disturbance in space. The influence of the disturbance of the space unit on its adjacent space unit of order k is denoted as $V(\overline{W}^k)$, as shown in

$$V\left(\overline{W}^k\right) = \rho_k\overline{W}^k\,(k = 1, 2, \ldots, k, \ldots, K). \tag{37}$$

The spatial propagation process of congestion can be summarized as a process in which the influence of local spatial units gradually spreads outwards through neighboring units. Congestion first spreads from spontaneously congested spatial units to neighboring spatial units and then from neighboring spatial units to second-order units. The continuous spread to the surroundings eventually leads to the proliferation and transformation of congestion. Therefore, the spatial propagation effects of local congestion can be calculated by formula (37), and the distribution of congestion spatial propagation effects under different spatial adjacency numbers can be investigated and then the spatial process of congestion propagation can be studied.

3.4.1. Propagation Effect of Congestion. Suppose that the space unit is congested and the speed of its first-order adjacent unit is disturbed through the adjacency relationship. The first-order propagation effect generated by the space

unit, that is, the influence on each adjacent unit can be represented by $V(\overline{W}^1)_{i,j}$ (j is the first-order adjacent space unit of i). Similarly, after congestion is propagated k times, the influence of spatial unit i on its k-order adjacent unit is expressed as $V(\overline{W}^k)_{i,j}$. Then, the ratio of the kth propagation effect to the total propagation effect is shown in

$$\mu_k = \frac{V\left(\overline{W}^k\right)_{i,j}}{\sum_{k=1}^{K} V\left(\overline{W}^k\right)_{i,j}}\#. \tag{38}$$

3.4.2. Interaction Degree Matrix between Spatial Units. The change of velocity perturbation of each space unit in the study area is the result of the combined effect of multiple space units. In order to quantify the degree of mutual influence between spatial units, the disturbance formed by the influence of spatial unit j by i is recorded as $v_{i,j}$ and then the degree of influence of spatial unit i on spatial unit j is calculated:

$$W = \begin{bmatrix} w_{1,1} & w_{1,2} & \cdots & w_{1,j} & \cdots & w_{1,n} \\ w_{2,1} & w_{2,2} & \cdots & w_{2,j} & \cdots & w_{2,n} \\ w_{i,1} & w_{i,2} & \cdots & w_{i,j} & \cdots & w_{i,n} \\ \vdots & \vdots & \ddots & \vdots & \ddots & \vdots \\ w_{n,1} & w_{n,2} & \cdots & w_{n,j} & \cdots & w_{n,n} \end{bmatrix}, \tag{39}$$

$$w_{i,j} = \frac{v_{i,j}}{\sum_{i=1}^{102} v_{i,j} \sum}, \tag{40}$$

$$v_{i,j} = \sum_{k=1}^{K} \rho_k\left(\overline{w}^k\right)_{i,j} y_i \quad . \tag{41}$$

3.4.3. Identification of Key Nodes. In the discipline of complex networks, nodes that are easily damaged and have a greater impact on other nodes are called key nodes. With reference to the definition of key nodes in a complex network, this paper proposes a method for identifying key nodes in the congestion evolution process of the entrance and exit areas: the space where the speed of the space unit is susceptible to influence and has a greater impact on the speed of adjacent space units. The unit is defined as the key node in the congestion evolution process of the entrance and exit area.

Based on the abovementioned definition of traffic congestion and related standards, "Urban Traffic Management Evaluation Index System" (2002, China), the spatial unit under the transmission effect is divided into 5 states: spontaneously congested units, heavily congested units, moderately congested units, lightly congested units, and immune units. The specific classification criteria are shown in Table 2.

The first of the above five traffic states is the congestion formed under the influence of its own factors, while the other four are under the comprehensive influence of the congestion propagation effect of neighboring units. When the disturbance rises sharply and reaches a certain threshold, the traffic state gradually changes from unblocked to congested, indicating that the propagation effect is the main reason for the decline in service level and even congestion in the entrance and exit areas.

Based on the method of judging the traffic state, this paper defines the space unit with a speed greater than 10 km/h and an impact on adjacent space units greater than 30% as a key node in the congested traffic state/process.

4. Results

4.1. Goodness-of-Fit Test. The goodness-of-fit test is conducted on the velocity disturbance sequence in the experimental area under the improved spatial autoregressive model. According to the parameter fitting results, the goodness-of-fit (R^2) value of the improved spatial autoregressive model is 0.7423, indicating that the model has a good fitting effect.

According to the test shown in Figure 3, divergence between the actual observed value and predicted value in each spatial unit is small and the actual observed value curve and the predicted value curve are very close, indicating the improved spatial autoregressive model can reasonably describe the trend of speed at various locations. In a nutshell, the model performs well in predicting the speed disturbance of each spatial unit and can truly and reasonably reflect the spatial correlation of the traffic of various units in the area.

4.2. Analysis on the Evolution Law of Congestion in the Entrance and Exit. Congestion evolution analysis, the method proposed in this paper, is used to study the evolution of congestion in the entrance and exit. Twenty sets of observed data whose traffic flow is 2000 pcu/h and entry rate is 20% are collected for research. By calculating the congestion propagation in the entrance and exit and the influence matrix of different spatial units, the key nodes of the evolution of congestion in the area can be perceived and its formation mechanism can be analyzed.

4.2.1. Analysis of Congestion Propagation in the Entrance and Exit. Based on the criteria in Table 2, the traffic of each spatial unit in the entrance and exit can be determined and the spatial distribution is shown in Figure 4. It can be seen from the distribution of various congestion units that the spread of local congestion is not isotropic; the frontage road to the entrance and exit of the parking lot is the culprit of local congestion, and the units where they are located are mostly the spontaneous congestion units; the congestion propagates to the inner lane and the downstream of the road segments from the spontaneous congestion units. The outer lane is affected most, and the affected area is also the largest; the middle lane and the inner lane are the least affected; and

Table 2: Definition of the traffic status of the space unit (unit: km/h).

Status	Disturbance range	Speed range	Description
Spontaneously congested unit			Congestion occurs first
Heavily congested unit	>20	<10	Vehicles are in a queue
Moderately congested unit	10~20	10~20	Low speed with a standstill
Lightly congested unit	0~10	20~30	Moderate speed with no standstill
Immune unit	≤0	>30	Faster speed in a free-flow state

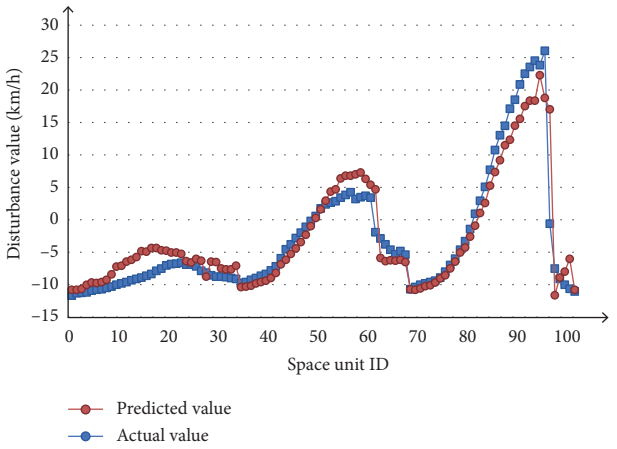

Figure 3: Comparison between the predicted value curve and actual observed value curve.

the downstream area of the entrance and exit and the upstream of the affected area are almost no longer affected.

In order to further explore the interaction between spatial units and understand the characteristics of congestion propagation, five spatial units with different traffic are selected and the distributions of congestion of spatial units of different orders are compared. The result is shown in Figure 5. It can be seen from the figure that the propagation whose spatial adjacency is within the fourth order accounts for more than 90% of the total propagation. Propagation gradually decreases as the spatial adjacency increases. This shows that when congestion happens in a spatial unit, its impact on the most adjacent spatial unit (first-order adjacent unit) is the greatest, and as the spatial scale increases, the impact decreases sharply.

4.2.2. Spatial Evolution Mechanism of Congestion in the Entrance and Exit. In order to further analyze the evolution mechanism of congestion in the entrance and exit, this paper calculates the influence matrix of spatial units based on the improved spatial autoregressive model and quantifies the degree of mutual influence between spatial units under the influence of congestion propagation. The spatial unit is regarded as the node, the mutual influence between the spatial units as the edge, and the degree of mutual influence as the weight, and a directed weighted network of the spatial units can be constructed, as shown in Figure 6.

It can be seen from Figure 6 that the directed weighted network of spatial units in the experimental area takes the shape of a "band," which is consistent with the above-mentioned attenuation characteristics of congestion propagation. To better analyze and study the evolution mechanism of congestion in the area, this paper divides the congestion evolution process into entrance and exit section area, transition area, and upstream area based on different spatial locations where the congestion happens. Figure 7 draws a directed weighted network for the three areas and uses the abstract network to analyze the evolution process of congestion.

(1) Section Area of the Entrance and Exit. The directed weighted network near the entrance and exit shows that affected by the parking behavior, there are significant differences in the weight values of the spatial units near the section. Based on the directed weighted network near the section (Figure 8), Figure 9 is drawn. All units in Figure 9 are spatial units in the section area of the entrance and exit; A, B, and C indicate Lane 1, Lane 2, and Lane 3, respectively, 1, 2, 3, 4, and 5 indicate adjacent spatial units from upstream to downstream of the road; C3, C4, and C5 are spontaneous congestion units, and other units are general units. It can be seen from the figure that the lateral interference on the spatial unit accounts for about 85% of the total in Lane 1 (outermost lane), and the lateral interference on the spatial unit accounts for 60% of the total in Lane 2 (middle lane). The main reason for the spontaneous congestion units in Lane 3 (innermost lane) is that the service capacity of the entrance and exit of the parking lot cannot meet the needs of parking and the entry time is prolonged due to the conflict between motor vehicles and nonmotorized vehicles. These ultimately make it impossible to ease the vehicles and cause congestion to propagate upstream.

(2) Transition Area. From the directed weighted network in the transition area (Figure 10) and the diagram of spatial units (Figure 11) (all the units in the figure are units in the transition area and all are general units, and the meanings of all the other symbols are the same as the preceding text), it can be seen that under the influence of the vehicle stagnation, the ratio of longitudinal interference to the total interference the spatial units receive in Lane 3 varies within the range of [0.5, 0.65], and the ratio of longitudinal interference to the total interference and the distance between the spatial units and the entrance and exit is inversely correlated. The ratio of the longitudinal interference to the total interference the spatial units receive on Lane 2 varies within the range of [0.35, 0.6], and the ratio of the lateral interference to the total interference the spatial units receive on Lane 2 varies within the range of [0.1, 0.45]. Moreover, the ratio of longitudinal interference to the total interference is positively correlated with the distance between the spatial units and the entrance and exit, and the ratio of lateral interference to the total interference is negatively correlated

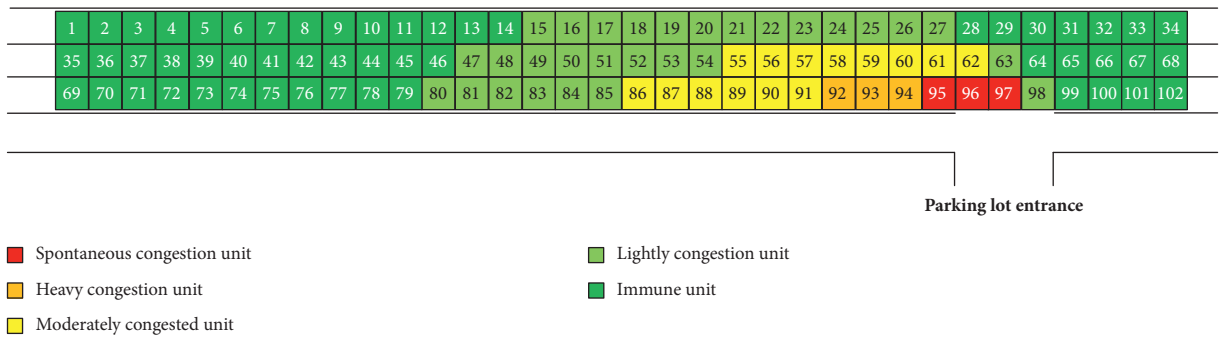

Figure 4: Distribution of the spatial unit.

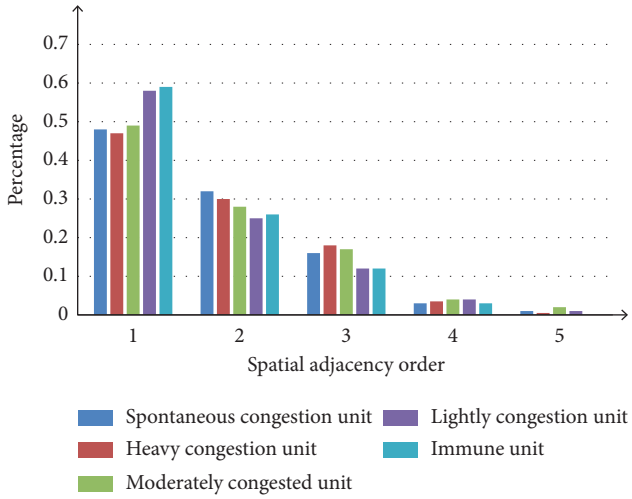

Figure 5: The attenuation process of spatial congestion propagation.

with the distance between the spatial units and the entrance and exit. This is because the spatial units in Lane 2 is affected by the combination of stagnation of vehicles in the same lane and lane changing of driving vehicles in Lane 3, and the speed is disturbed. As the distance increases, the impact of lane changing on Lane 2 gradually decreases, and the impact of stagnation on the upstream units gradually becomes the main factor, which is manifested by the gradual increase in the weight value of the units in Lane 2. The longitudinal interference the spatial units receive on Lane 1 accounts for about 65% of the total, which is mainly caused by the vehicles changing lanes.

(3) Upstream Area. The directed weighted network of the spatial units in the upstream area of the entrance and exit is shown in Figure 12. The weight value between the spatial units in the upstream area tends to be stable, which means that the congestion is propagated upstream in the same pattern. The relationship between spatial units is illustrated by Figure 13 (all the units in the figure are units in the upstream area and all are general units, and the meanings of all the other symbols are the same as the preceding text). It can be seen from the figure that the lateral interference the spatial units receive in Lane 1 accounts for more than 90% of the total. The main reason for this phenomenon is that the vehicles in Lane 1 rarely stagnate, and the spatial units are mainly affected by "friction effect"; in Lane 2, the lateral interference the spatial units receive in Lane 2 is about 60%. This is because the intermittent queuing of vehicles parked near the entrance and exit causes the vehicles in the upstream area to stagnate. Therefore, the mutual influence between the spatial units in the same lane is relatively high. Lane 3 is the lane directly connected to the entrance and exit. Due to the combination of frequent queuing, following the traffic flow and lane changing of parked vehicles, the longitudinal and lateral interferences the spatial units receive in Lane 3 are both about 50%.

To sum up, from the perspective of the impact value, the congestion propagation is the strongest in the frontage road to entrance and exit of the parking lot, where the congestion first happens; there is moderate propagation in the transition area, the main area where congested vehicles stagnate; congestion propagation is weak in the downstream area, stagnation of vehicles is barely seen, and there is a relatively fast-flowing traffic. From the perspective of the proportion, from the frontage road to the transition area and then to the upstream area, the proportion of longitudinal interference gradually increases, while the proportion of lateral interference gradually decreases. This shows that the lateral propagation of congestion attenuates faster than longitudinal propagation.

4.2.3. Key Congestion Nodes. In order to further analyze the relationship between the location and number of key nodes in the process of congestion evolution and the traffic volume of the road segments and the entry rate, this paper calculates the location of key nodes of congestion propagation when the traffic volume is 1500 pcu/h, 2000 pcu/h, and 2500 pcu/h, respectively, and when the entry rate of parked vehicles stands at 15%, 20%, and 25%, respectively (as shown in Table 3). Obviously, the traffic volume and the entry rate are positively correlated with the number of key nodes. As the traffic volume and the entry rate increase, key nodes spread from the outer lane to the inner lane and from the frontage road to the entrance and exit of the parking lot to the upstream area. Further comparative analysis shows that when the traffic volume is 1500 pcu/h, the change of the entry rate does not have a significant impact on the number of key nodes; when the traffic volume increases to 2000 pcu/h (especially when it increases to 2500 pcu/h), the number of

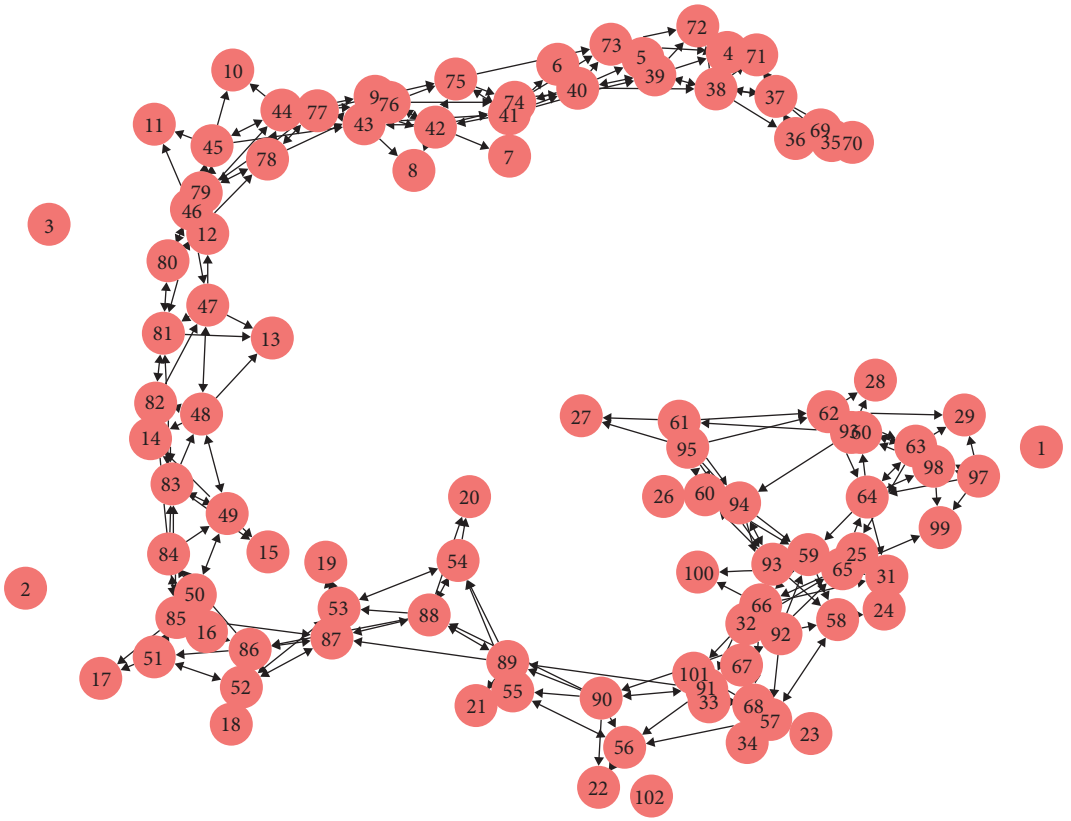

Figure 6: Directed weighted network of the entrance and exit.

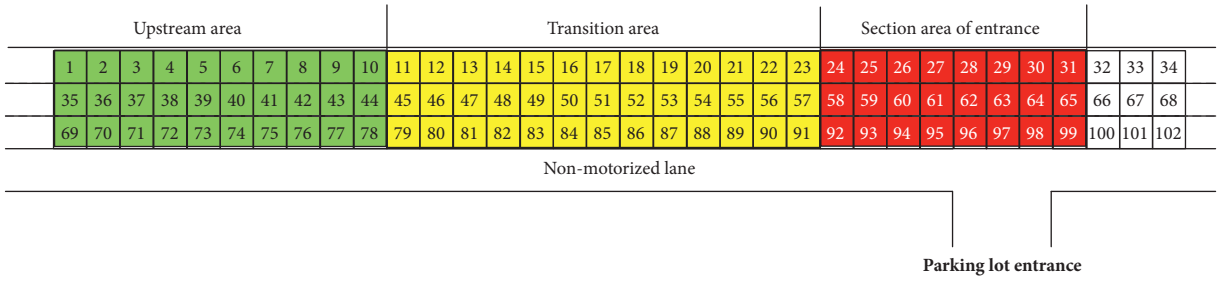

Figure 7: Diagram of the division of the entrance and exit.

key nodes increases significantly along with the increase in the entry rate, which shows that the impact of the entry rate on the key nodes is enhanced as the traffic volume of the road segments increases.

The analysis suggests that the degree, distribution, and number of congestion of spatial units in the entrance and exit are constantly changing. When the traffic volume of the road segments and entry rate are high, the degree and number of congestion of the spatial units of the entrance and exit will increase significantly, and vice versa. However, for each specific unit, whether it will become a congestion unit is not determined solely by the traffic volume or the entry rate, but by the combination of the traffic volume, the entry rate, and the location of the spatial unit. In the directed weighted network in the entrance and exit, some spatial units (key nodes under the effect of congestion propagation) quickly evolve into congestion units because of greater turbulence caused by the increase in traffic volume or entry rate. However, some units are less or not susceptible to the increase in traffic volume or entry rate. Therefore, in daily traffic management, the key nodes in the evolution process should be eased; for spontaneous congestion units, by improving the service capacity of entrances and exits and reducing the entry time of parked vehicles, the impact of spontaneous congestion units on adjacent units can be reduced; in terms of the key nodes under the influence of propagation, reducing stagnation of vehicles can alleviate the longitudinal propagation of congestion; in addition, guiding vehicles to enter the parking lot from other entrances with facilities such as parking grading guidance screens to reduce entry rate improve the frontage roads to the entrances and exits and enhance the quality of travel for citizens.

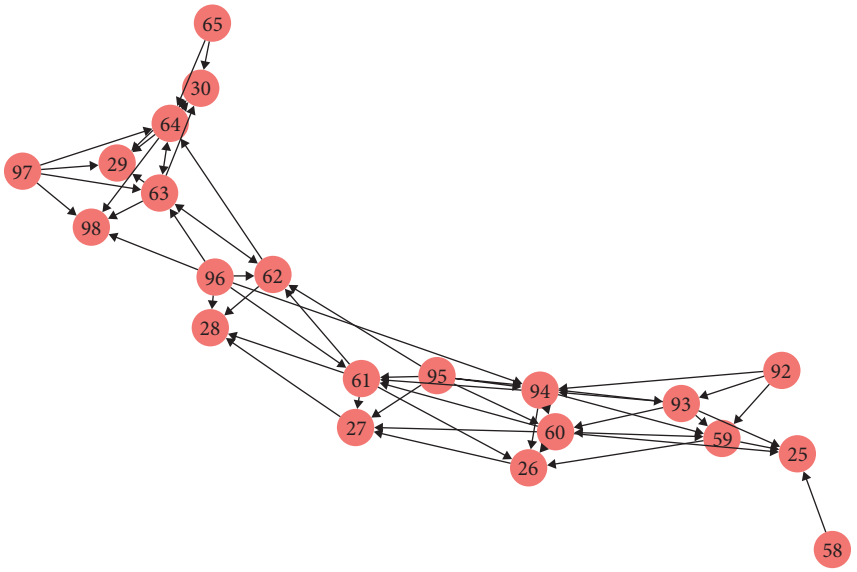

Figure 8: Diagram of a directed weighted network in the section area of the entrance and exit.

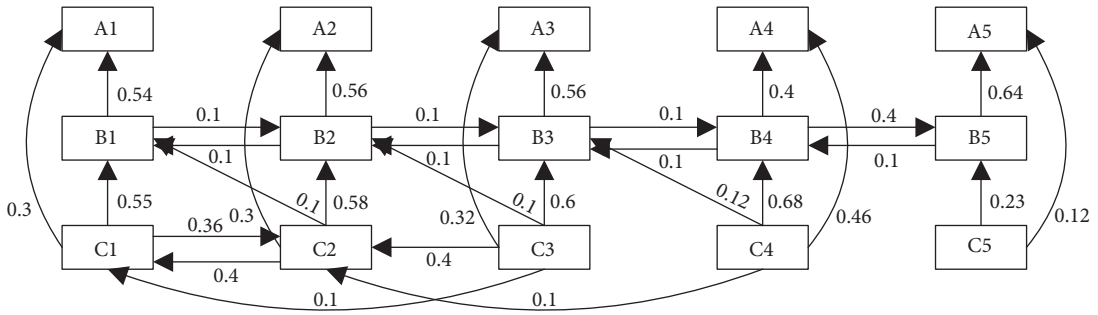

Figure 9: The diagram of spatial units in the section area of the entrance and exit.

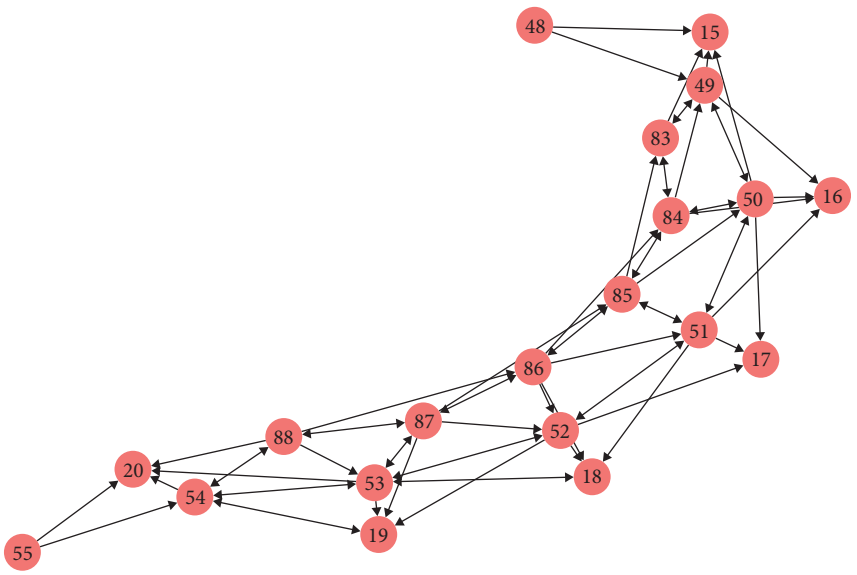

Figure 10: Diagram of a directed weighted network in the transition area.

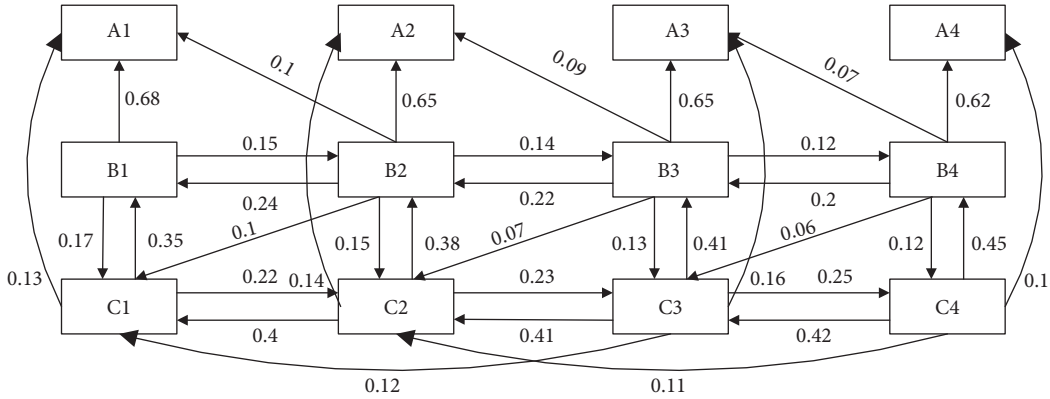

Figure 11: The diagram of spatial units in the transition area.

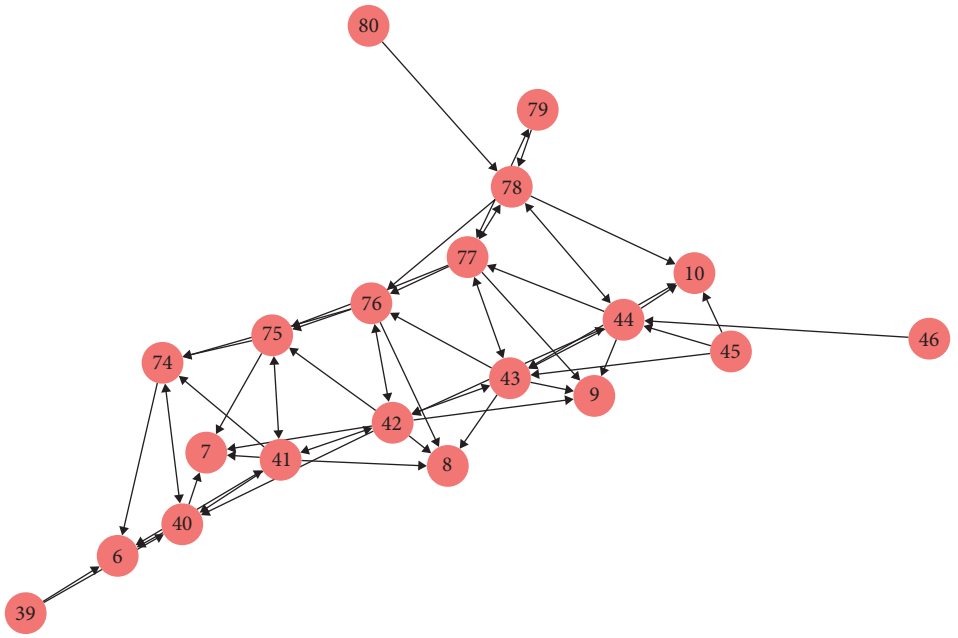

Figure 12: Diagram of a directed weighted network in the upstream area.

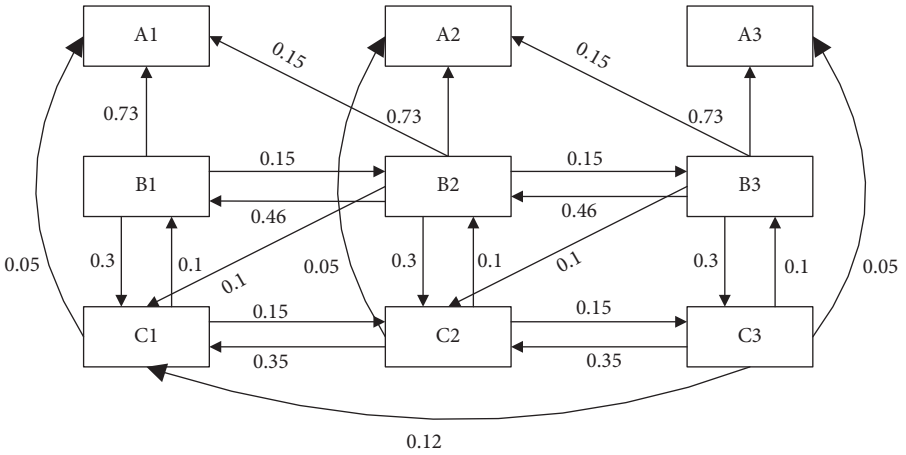

Figure 13: The diagram of spatial units in the upstream area.

Table 3: Key nodes of congestion propagation.

Traffic flow (±100 pcu/h)	Entry rate (±5 (%))	Key nodes
1500	15	95, 96, 97
	20	95, 96, 97
	25	93, 94, 95, 96, 97, 61, 62
2000	15	92, 93, 94, 95, 96, 97, 58, 59, 60, 61, 62
	20	89, 90, 91, 92, 93, 94, 95, 96, 97, 57, 58, 59, 60, 61, 62
	25	86, 87, 88, 89, 90, 91, 92, 93, 94, 95, 96, 97, 54, 55, 56, 57, 58, 59, 60, 61, 62
2500	15	88, 89, 90, 91, 92, 93, 94, 95, 96, 97, 54, 55, 56, 57, 59, 60, 61, 62
	20	83, 84, 85, 86, 87, 88, 89, 90, 91, 92, 93, 94, 95, 96, 97, 51, 52, 53, 54, 55, 56, 57, 58, 59, 60, 61, 62
	25	76, 77, 78, 79, 80, 81, 82, 83, 84, 85, 86, 87, 88, 89, 90, 91, 92, 93, 94, 95, 96, 97, 47, 48, 49, 50, 51, 52, 53, 54, 55, 56, 57

5. Conclusions and Discussion

This paper starts with studying the spatial evolution pattern of congestion propagation in the entrance and exit of a parking lot. First, it discusses the shortcomings of traditional spatial autoregressive model and proposes an improved robust spatial autoregressive model based on the actual characteristics of the traffic flow in the entrance and exit. Second, it constructs a smooth spatial adjacency matrix based on the principal component analysis and designs a parameter estimation method based on partial least squares. Third, it selects the frontage road to entrance and exit of a typical parking lot for research, and the fitting result (R^2 is 0.7423) shows that the model has a good fitting performance for the velocity disturbance sequence of the spatial units. Fourth, by identifying and observing the distribution of different types of congestion units in the research section, the mechanism of congestion formation and the main propagation direction are analyzed. Finally, it explores and analyzes the congestion propagation and the spatial evolution mechanism of the congestion in the experimental area. The results show that as the spatial scale increases, the congestion propagation decreases sharply, and spatial adjacency within the fourth order can account for more than 90% of the propagation; the frontage road to the entrance and exit is the place where the congestion first happens; the congestion gradually attenuates as it propagates to the inner lane and the upstream of the road segments; the lateral congestion propagation attenuates faster, so the area affected by congestion is mainly distributed in the outermost lane. In summary, the proposed method for analyzing the spatial propagation characteristics of traffic congestion can be better applied to the frontage roads of parking facilities. The results of the case analysis show that for the local traffic congestion at the entrance and exit, the relevant departments should proceed from a holistic perspective to accurately monitor and orderly channel the key space nodes. The conclusions are of great theoretical and practical significance for improving the frontage roads to the entrances and exits of parking facilities and the quality of travel for citizens.

Data Availability

The measured data used to support the findings of this study are included within the article and the supplementary files.

Conflicts of Interest

The authors declare no conflicts of interest.

Acknowledgments

This work was supported by Research Planning Fund for Humanities and Social Sciences of the Ministry of Education (19YJAZH011), Support for the Open Project of Key Laboratory of Intelligent Traffication Technology and Traffication Industry (F262019016), Science and Technology Project of Traffication Department of Jiangsu Provincial Department of Communications (KY2018049), Jiangsu Provincial Department of Science and Technology Industry-University-Research Cooperation Project "Traffic Safety-Oriented Intelligent Supervision and Decision Support System Platform Research and Development" (BY2019263), and the Key Project of Transportation Science and Technology Achievement & Transformation of Jiangsu Province (2019Z01).

Supplementary Materials

The following is a concise description to the supplementary file. The data include our observation records of the frontage road section of the parking lot of the West Affiliated Hospital of Yangzhou University, when the entry rate is about 20% and the traffic flow is around 2000 pcu/h. The columns of data represent the labels of 13 groups of observations; the indexes represent the IDs of the spatial units, and values represent the average values of the instantaneous speed of 100 observations, recorded every 3 s for 5 min, for each group of each unit. (*Supplementary Materials*)

References

[1] China Statistical Yearbook, 2021, https://www.stats.gov.cn/tjsj/ndsj/.

[2] J. Chen and G. Yang, "Off-street parking," in *International Encyclopedia of Transportation*, R. Vickerman and R. Vickerman, Eds., Elsevier, Oxford, UK, 2021.

[3] T. Shen, Y. Hong, M. M. Thompson, J. Liu, X. Huo, and L. Wu, "How does parking availability interplay with the land use and affect traffic congestion in urban areas? The case study of Xi'an, China," *Sustainable Cities and Society*, vol. 57, Article ID 102126, 2020.

[4] P. Zhao, H. Guan, H. Wei, and S. Liu, "Mathematical modeling and heuristic approaches to optimize shared parking resources: a case study of Beijing, China," *Transportation Research Interdisciplinary Perspectives*, vol. 9, Article ID 100317, 2021.

[5] X. Cai, L. Lu, J. J. Lu, and W. Lin, "Impacts of access density on traffic capacity of arterial roads," in *Proceedings of the 4th International Conference on Transportation Engineering*, pp. 359–364, Chengdu, China, October 2013.

[6] J. Zhao, P. Li, and X. Zhou, "Capacity estimation model for signalized intersections under the impact of access point," *PLoS One*, vol. 11, no. 1, Article ID e0145989, 2016.

[7] C. Jiang and L. Lu, "Influences of access density of minor roads on arterial speed variance by TSIS," in *Proceedings of the 4th International Conference on Transportation Engineering*, Chengdu, China, October 2013.

[8] J. A. Bonneson, "Delay to major-street through vehicles due to right-turn activity," *Transportation Research Part A: Policy and Practice*, vol. 32, no. 2, pp. 139–148, 1998.

[9] X. Hu, T. Liu, X. Hao, Z. Su, and Z. Yang, "Research on the influence of bus bay on traffic flow in adjacent lane: simulations in the framework of Kerner's three-phase traffic theory," *Physica A: Statistical Mechanics and its Applications*, vol. 563, Article ID 125495, 2021.

[10] M. Johari, M. Keyvan-Ekbatani, and D. Ngoduy, "Impacts of bus stop location and berth number on urban network traffic performance," *IET Intelligent Transport Systems*, vol. 14, no. 12, pp. 1546–1554, 2020.

[11] S. Liang, M. Ma, S. He, H. Zhang, and Z. Tang, "Influence of bus stop location on traffic flow," *Proceedings of the Institution of Civil Engineers-Municipal Engineer*, vol. 174, no. 1, pp. 24–31, 2021.

[12] F. Han, Y. Han, M. Ma, and D. Zhao, "Research on traffic wave characteristics of bus in and out of stop on urban expressway," *Procedia Engineering*, vol. 137, pp. 309–314, 2016.

[13] P. Bansal, R. Agrawal, and G. Tiwari, "Impacts of bus-stops on the speed of motorized vehicles under heterogeneous traffic conditions: a case-study of Delhi, India," *International Journal of Transportation Science and Technology*, vol. 3, no. 2, pp. 167–178, 2014.

[14] P. Raj, G. Asaithambi, and A. U. Ravi Shankar, "Effect of curbside bus stops on passenger car units and capacity in disordered traffic using simulation model," *Transportation Letters*, vol. 2, 2020.

[15] Y. Cao, Z. Z. Yang, and Z. Y. Zuo, "The effect of curb parking on road capacity and traffic safety," *European Transport Research Review*, vol. 9, no. 1, 2017.

[16] Z. Mei and J. Chen, "Modified motor vehicles travel speed models on the basis of curb parking setting under mixed traffic flow," *Mathematical Problems in Engineering*, vol. 2012, Article ID 351901, 14 pages, 2012.

[17] S. Salini and R. Ashalatha, "Analysis of traffic characteristics of urban roads under the influence of roadside frictions," *Case Studies on Transport Policy*, vol. 8, no. 1, pp. 94–100, 2020.

[18] M. Patkar and A. Dhamaniya, "Effect of on-street parking on effective carriageway width and capacity of urban arterial roads in India," *European Transport-Trasporti Europei*, no. 73, 2019.

[19] K. Seggerman and K. Williams, "Managing the indirect impacts of bypasses on small and medium-sized communities in Florida," *Transportation Research Record: Journal of the Transportation Research Board*, vol. 2453, no. 1, pp. 46–53, 2014.

[20] J. Kim and H. S. Mahmassani, "Spatial and temporal characterization of travel patterns in a traffic network using vehicle trajectories," *Transportation Research Part C: Emerging Technologies*, vol. 59, pp. 375–390, 2015.

[21] B. Bae, Y. Liu, L. D. Han, and H. Bozdogan, "Spatio-temporal traffic queue detection for uninterrupted flows," *Transportation Research Part B: Methodological*, vol. 129, pp. 20–34, 2019.

[22] D. Ni and J. D. Leonard, "A simplified kinematic wave model at a merge bottleneck," *Applied Mathematical Modelling*, vol. 29, no. 11, pp. 1054–1072, 2005.

[23] G. F. Newell, "A moving bottleneck," *Transportation Research Part B: Methodological*, vol. 32, no. 8, pp. 531–537, 1998.

[24] G. Gentile, "Using the general link transmission model in a dynamic traffic assignment to simulate congestion on urban networks," *Transportation Research Procedia*, vol. 5, pp. 66–81, 2015.

[25] S. Kurata and T. Nagatani, "Spatio-temporal dynamics of jams in two-lane traffic flow with a blockage," *Physica A*, vol. 318, no. 3, pp. 537–550, 2003.

[26] C. Wright and P. Roberg, "The conceptual structure of traffic jams," *Transport Policy*, vol. 5, no. 1, pp. 23–35, 1998.

[27] M. Saeedmanesh and N. Geroliminis, "Dynamic clustering and propagation of congestion in heterogeneously congested urban traffic networks," *Transportation Research Part B: Methodological*, vol. 105, pp. 193–211, 2017.

[28] J. Song, C. Zhao, S. Zhong, T. A. S. Nielsen, and A. V. Prishchepov, "Mapping spatio-temporal patterns and detecting the factors of traffic congestion with multi-source data fusion and mining techniques," *Computers, Environment and Urban Systems*, vol. 77, Article ID 101364, 2019.

[29] B. Alkouz and Z. Al Aghbari, "SNSJam: road traffic analysis and prediction by fusing data from multiple social networks," *Information Processing & Management*, vol. 57, no. 1, Article ID 102139, 2020.

[30] Y. Song, X. Liang, Y. Zhu, and L. Lin, "Robust variable selection with exponential squared loss for the spatial autoregressive model," *Computational Statistics & Data Analysis*, vol. 155, Article ID 107094, 2021.

[31] S. P. Zhou and J. J. Zhang, "Quasi-maximum likelihood estimations and applications for spatial dynamic autoregressive panel model with fixed effects," *Systems Engineering-Theroy & Practice*, vol. 41, no. 1, pp. 45–57, 2021.

[32] F. Han and F. Sui, "Effect of global moran's I and space-time permutation scanning method in shanghai metro traffic based on ecological transportation system," *Ekoloji*, vol. 28, pp. 4741–4749, 2019.

[33] H. Rong, A. P. Teixeira, and C. Guedes Soares, "Spatial correlation analysis of near ship collision hotspots with local maritime traffic characteristics," *Reliability Engineering & System Safety*, vol. 209, Article ID 107463, 2021.

[34] A. Soltani and S. Askari, "Exploring spatial autocorrelation of traffic crashes based on severity," *Injury*, vol. 48, no. 3, pp. 637–647, 2017.

[35] T. Ban, T. Usui, and T. Yamamoto, "Spatial autoregressive model for estimation of visitors' dynamic agglomeration patterns near event location," *Sensors*, vol. 21, no. 13, p. 4577, 2021.

[36] X. Zhang, G. Chen, J. Wang, M. Li, and L. Cheng, "A GIS-based spatial-temporal autoregressive model for forecasting marine traffic volume of a shipping network," *Scientific Programming*, vol. 2019, Article ID 2345450, 14 pages, 2019.

[37] Y. Wang, Y. Yuan, X. Guan et al., "Collaborative two-echelon multicenter vehicle routing optimization based on state-

space-time network representation," *Journal of Cleaner Production*, vol. 258, Article ID 120590, 2020.

[38] Y. Wang, S. Peng, and M. Xu, "Emergency logistics network design based on space-time resource configuration," *Knowledge-Based Systems*, vol. 223, Article ID 107041, 2021.

[39] Y. Wang, X. Ma, Z. Li, Y. Liu, M. Xu, and Y. Wang, "Profit distribution in collaborative multiple centers vehicle routing problem," *Journal of Cleaner Production*, vol. 144, pp. 203–219, 2017.

[40] Y. Wang, S. Peng, X. Zhou, M. Mahmoudi, and L. Zhen, "Green logistics location-routing problem with eco-packages," *Transportation Research Part E: Logistics and Transportation Review*, vol. 143, Article ID 102118, 2020.

[41] N. G. Álvarez, B. Adenso-Díaz, and L. Calzada-Infante, "Maritime traffic as a complex network: a systematic review," *Networks and Spatial Economics*, pp. 1–31, 2021.

[42] L. Siozos-Rousoulis, D. Robert, and W. Verbeke, "A study of the U.S. domestic air transportation network: temporal evolution of network topology and robustness from 2001 to 2016," *Journal of Transportation Security*, 2021.

[43] Y. Sui, F. Shao, X. Yu, R. Sun, and S. Li, "Public transport network model based on layer operations," *Physica A: Statistical Mechanics and its Applications*, vol. 523, pp. 984–995, 2019.

[44] H.-Z. Lin and J. Wei, "Optimal transport network design for both traffic safety and risk equity considerations," *Journal of Cleaner Production*, vol. 218, pp. 738–745, 2019.

[45] Y. Sui, F.-j. Shao, R.-c. Sun, and S.-j. Li, "Space evolution model and empirical analysis of an urban public transport network," *Physica A: Statistical Mechanics and its Applications*, vol. 391, no. 14, pp. 3708–3717, 2012.

[46] R. Khalid, M. K. M. Nawawi, L. A. Kawsar, N. A. Ghani, A. A. Kamil, and A. Mustafa, "Optimal routing of pedestrian flow in a complex topological network with multiple entrances and exits," *International Journal of Systems Science*, vol. 51, no. 8, pp. 1325–1352, 2020.

[47] YOLOV5-deepsort-pytorch, 2021, https://github.com/topics/yolov5-deepsort-pytorch.

[48] X. Chen, L. Qi, Y. Yang et al., "Video-based detection infrastructure enhancement for automated ship recognition and behavior analysis," *Journal of Advanced Transportation*, vol. 2020, Article ID 7194342, 12 pages, 2020.

[49] X. Chen, Z. Li, Y. Yang, L. Qi, and R. Ke, "High-resolution vehicle trajectory extraction and denoising from aerial videos," *IEEE Transactions on Intelligent Transportation Systems*, vol. 22, no. 5, pp. 3190–3202, 2021.